AEM
Journals.ASM.org

Hha Controls *Escherichia coli* O157:H7 Biofilm Formation by Differential Regulation of Global Transcriptional Regulators FlhDC and CsgD

Vijay K. Sharma,[a] Bradley L. Bearson[b]

Food Safety and Enteric Pathogens Research Unit, National Animal Disease Center, ARS-USDA, Ames, Iowa, USA[a]; Agroecosystems Management Research Unit, National Laboratory for Agriculture and the Environment, ARS-USDA, Ames, Iowa, USA[b]

Although molecular mechanisms promoting adherence of enterohemorrhagic *Escherichia coli* (EHEC) O157:H7 on epithelial cells are well characterized, regulatory mechanisms controlling biofilm formation are not fully understood. In this study, we demonstrate that biofilm formation in EHEC O157:H7 strain 86-24 is highly repressed compared to that in an isogenic *hha* mutant. The *hha* mutant produced large quantities of biofilm compared to the wild-type strain at 30°C and 37°C. Complementation of the *hha* mutant reduced the level of biofilm formation to that of the wild-type strain, indicating that Hha is a negative regulator of biofilm production. While swimming motility and expression of the flagellar gene *fliC* were significantly reduced, the expression of *csgA* (encoding curlin of curli fimbriae) and the ability to bind Congo red were significantly enhanced. The expression of both *fliC* and *csgA* and the phenotypes of motility and curli production affected by these two genes, respectively, were restored to wild-type levels in the complemented *hha* mutant. The *csgA* deletion abolished biofilm formation in the *hha* mutant and wild-type strain, and *csgA* complementation restored biofilm formation to these strains, indicating the importance of *csgA* and curli in biofilm formation. The regulatory effects of Hha on flagellar and curli gene expression appear to occur via the induction and repression of FlhDC and CsgD, as demonstrated by reduced *flhD* and increased *csgD* transcription in the *hha* mutant, respectively. In gel shift assays Hha interacted with *flhDC* and *csgD* promoters. In conclusion, Hha regulates biofilm formation in EHEC O157:H7 by differential regulation of FlhDC and CsgD, the global regulators of motility and curli production, respectively.

Escherichia coli O157:H7 (referred to herein as O157) is the most frequent cause of sporadic and multiperson outbreaks of hemorrhagic colitis and hemolytic uremic syndrome (HUS) in humans (1). O157 uses diverse sets of adherence mechanisms to colonize intestinal epithelial cells and to produce biofilms on abiotic and biotic surfaces (2–5). Intimate adherence of O157 to bovine and human intestinal epithelial cells results in the formation of characteristic attaching and effacing (A/E) lesions and requires the LEE (locus of enterocyte effacement)-encoded type III secretion system and adherence factors (6).

On the other hand, formation of biofilms in both pathogenic and nonpathogenic *E. coli* strains requires differential and temporal expression of extracellular matrix components that facilitate a transition from an independent planktonic state to an organized multicellular community living within a highly structured extracellular matrix (7). One prominent component of this matrix is the adhesive fimbrial structures referred to as curli, which are thin, coiled, highly aggregative fibers of various lengths that protrude from the bacterial cell surface (8). Besides binding Congo red dye, the adhesive properties of curli enable *E. coli* to bind various host proteins, colonize animal tissues, activate the immune system, and produce biofilms on inanimate surfaces (8–13). Curli fimbriae are composed primarily of the protein curlin, encoded by the *csgA* gene of the *csgBAC* operon (14).

In addition to curli, flagella are required for the initial stages of biofilm formation in *E. coli*, as demonstrated by the inability of motility-deficient mutants to produce biofilms (15). However, motility is not required for biofilm formation by all *E. coli* strains, such as nonflagellated enteroaggregative *E. coli* strains that are as capable of producing biofilms like the flagellated wild-type strains on glass and plastic surfaces (16). The flagellar requirement is also bypassed in *E. coli* strains that overproduce curli or harbor conjugative F plasmids (17, 18).

In *E. coli*, flagellum-dependent swimming motility and curli-mediated adherence to solid surfaces during biofilm formation are regulated by a complex network of regulatory cascades. The *csgD* gene of the *csgDEFG* is a FixJ/LuxR family of transcriptional regulators that along with sigma factors RpoS-RpoE forms a regulatory cascade for activation of curli gene expression and biofilm production (19). The regulation of flagellar gene expression in *E. coli* is controlled by the master regulator FlhDC (class I flagellar operon) and RpoF cascade for activating the expression of class II and III flagellar genes (20–22). FliC, which represents the major structural protein of the *E. coli* flagellum, is encoded by the class III flagellar gene *fliC* (21, 22).

The expression of *flhDC* and *csgD* is controlled by a variety of physiological and environmental cues that activate or repress transcriptional regulators of the *flhDC* and *csgD* operons (19, 23–25). For example, flagellar genes are expressed under conditions favoring rapid growth and expression of curli is enhanced during slow growth or stationary phase, nutritional deprivation, low temperature, low osmolarity, and oxidative stress (26–30). Tempera-

Received 28 September 2012 **Accepted** 25 January 2013
Published ahead of print 1 February 2013
Address correspondence to Vijay K. Sharma, vijay.sharma@ars.usda.gov.

doi:10.1128/AEM.02998-12

TABLE 1 Bacterial strains and plasmids[a]

E. coli strain or plasmid	Genotype and description	Source or reference(s)
Strains		
E. coli O157:H7 strain 86–24	stx_2^+ and streptomycin resistant	46, 77
86–24 Δ*hha*	86–24 deleted of *hha*	44
86–24 Δ*csgA*	86–24 deleted of *csgA*	This study
86–24 Δ*hha* Δ*csgA*	86–24 deleted of *hha csgA*	This study
TOP 10	F$^-$ *mcrA* Δ(*mrr-hsdRMS-mcrBC*) ϕ80*lacZ*ΔM15 Δ*lacX74 recA1 araD139* Δ(*ara-leu*)*7697 galU galK rpsL* (Str^r) *endA1 nupG* λ	Invitrogen
BL21	F$^-$ *ompT hsdS*(r_B^- m_B^-) *gal dcm*	Amersham Biosciences
Plasmids		
pKD46	Recombineering vector	49
pCP20	FLP recombinase vector	51
pCR2.1	Cloning vector	Invitrogen
pSM197R		44
pSM569	*csgA*-complementing plasmid (pCR2.1 containing a cloned copy of *csgBAC*)	This study
pSM138	Hha expression plasmid (pGEX4T-3 containing *hha* ORF)	44

[a] See Materials and Methods for a detailed description of bacterial strains and plasmids listed in this table.

ture was one of the first environmental cues recognized to affect the expression of global regulatory cascades that redirect bacterial cells to form biofilms by upregulating production of curli and extracellular polysaccharides along with bacterial cell surface-associated proteins and nucleic acids (19, 24, 30–36). The selective expression of desired sets of genes in response to temperature cues is a common theme among commensal and pathogenic bacterial species for conserving energy and ensuring their survival and persistence in a specific niche as well as transmission to a new host or locale (28, 29, 37). A recent study comparing the global gene expression profiles of *E. coli* K-12 grown at 37°C or 30°C showed elevated expression of metabolic pathways, such as uptake and utilization of amino acids, carbohydrates, and iron needed for rapid growth at 37°C (29). On the other hand, growth of *E. coli* at low temperatures (≤32°C) resulted in reduced expression of genes affecting energy metabolism and amino acid biosynthesis and uptake, gene expression changes linked to slow growth and biofilm formation (30, 33). A recent review summarized how bacterial pathogens use the mammalian host body temperature of 37°C as a cue for growth and to regulate the expression of virulence genes and to cause disease in infected hosts (37).

Biofilms have been shown to enhance persistence of foodborne bacterial pathogens, including O157, on meat-processing equipment and surfaces in animal slaughter and meat packing plants due to their ability to produce biofilms or be recruited into mixed-community biofilms in mammalian intestines (38, 39). The importance of curli as important virulence determinants in human disease has been confirmed by reports demonstrating that many clinical isolates of *E. coli*, including those isolated from sepsis patients showing anti-curli antibodies in their blood and from patients who had developed HUS due to infection with nonmotile O157, expressed curli at 28°C and 37°C and showed enhanced adherence to epithelial cells (9, 40). However, the regulatory networks enabling expression of curli and production of biofilms by O157 in response to environmental factors, such as temperature, and host factors are not fully understood. In a recent study, we reported that SdiA, a LuxR homologue, acts as a repressor of flagellar and curli gene expression, while Hha represses curli but induces flagellar gene expression (41). The *hha* mutant showed enhanced biofilm formation relative to that of the *sdiA* mutant, indicating that the reduced motility and increased curli production are essential for biofilm formation at 30°C. Hha, originally identified as a negative regulator of hemolysin expression in *E. coli* strains, has also been demonstrated to act as a negative regulator of LEE expression and LEE-mediated adherence of O157 to epithelial cells (42–44).

Since low temperatures (≤30°C) are considered the norm for bacterial biofilm production (8, 28, 30), the major objectives of the present study were to determine whether the *hha* mutant that produces increased amounts of biofilms at 30°C (41) would do the same at 37°C through increased transcriptional levels of *csgA* resulting in the increased production of curli fimbriae. In addition, we wanted to determine the importance of curli fimbriae to and correlate relative effects of reduced motility of the *hha* mutant due to reduced *fliC* expression (41) on biofilm formation at 37°C and 30°C. And finally, we were interested in determining if *hha*-mediated differential regulation of *csgA* and *fliC*, which determines the quantity of biofilm being produced, occurs through the direct transcriptional regulation by Hha of FlhDC and CsgD, the master regulators of *fliC* and *csgA* expression, respectively.

MATERIALS AND METHODS

Bacterial strains, culture media, and growth conditions. Table 1 lists the bacterial strains and plasmids used in this study. *Escherichia coli* O157:H7 strain 86-24 (46) was used as the wild-type parent strain for constructing isogenic mutants. All *E. coli* strains were cultivated in Luria-Bertani broth (LB) or LB (Becton, Dickinson Companies, Sparks, MD) containing 1.5% agar (Sigma-Aldrich, St. Louis, MO). LB used contained 1% NaCl. YESCA broth (47, 48) was used for growth of bacterial strains to isolate RNA and for biofilm assays. YESCA agar (1.5% agar) was used to assess Congo red binding of bacterial strains. Swimming motility was determined on motility agar prepared by adding Noble agar (Becton, Dickinson) to YESCA broth at a final concentration of 0.33%. Media were supplemented with antibiotics at the following final concentrations: streptomycin, 100 mg liter^{-1}; kanamycin, 50 mg liter^{-1}; and carbenicillin, 100 mg liter^{-1}. The dyes Congo red and Coomassie brilliant blue G-250 were used at 40 μg ml^{-1} and 15 μg ml^{-1}, respectively.

Determination of bacterial generation times. Bacterial strains were grown overnight with shaking (200 rpm) at 37°C in YESCA broth containing carbenicillin at 100 μg^{-1} ml (YESCA-Carb). The overnight cultures were diluted 1:100 in YESCA-Carb, and after the addition of 300 μl of the diluted suspension to the wells of a 120-well Honeycomb 2 plate, the

TABLE 2 Primers used for PCR and QRT-PCR

Primer[c]	Nucleotide sequence[a]	Location[b]
fliC$_F$ (RT-PCR)	TTAGCTGCCACCCTTCATG	2700535–2700517
fliC$_R$ (RT-PCR)	TCGTCAAGTTGCCTGCATC	2700385–2700403
fliC$_P$ (RT-PCR)	TCTACGTATGCCTGGCTTCCACCG	2700405–2700428
csgA$_F$ (RT-PCR)	TACTATTACCCAGCATGGTGG	1548878–1548898
csgA$_R$ (RT-PCR)	CAAGAGTGGCGCTGTTACC	1548984–1548966
csgA$_P$ (RT-PCR)	CCACGTTGGGTCAGATCGATTGAG	1548962–1548938
flhDC$_F$ (RT-PCR)	ACAACATTAGCGGCACTGAC	2655207–2655188
flhDC$_R$ (RT-PCR)	AGAGTAATCGTCTGGTGGCTG	2655107–2655124
flhDC$_P$ (RT-PCR)	AAACGGAAGTGACAAACCAGCTGATTG	2655131–2655158
csgD$_F$ (RT-PCR)	CGCTGGCAATTACAGGAAAATTAC	1547324–1547301
csgD$_R$ (RT-PCR)	CTTTTTATCCGCTTCCATCATATCC	1547224–1547248
csgD$_P$ (RT-PCR)	ATATTCAACGTTCTCTGGACGATATCTCTTCAGGCT	1547297–1547262
rpoA$_F$ (RT-PCR)	GGCTTGACGATTTCGACATC	4242887–4242906
rpoA$_R$ (RT-PCR)	GGTGAGAGTTCAGGGCAAAG	4242997–4242978
rpoA$_P$ (RT-PCR)	TGAAGTTATTCTTACCTTGAATAAATCTGGCATTG	4242976–4242942
csgBAC$_F$	AACAAAAAAAGAAAAATACAACGC	1548016–1548039
csgBAC$_R$	GATCTCTAGATCTGAAGAGGGCGGCCATTG	1549511–1549492
flhDC$_F$ (promoter)	GATCGTCGACGTGCGCAACATCCCATTTCG	5655748- 5655729
flhDC$_R$ (promoter)	GATCAGATCTGTATGCATTATTCCCACCCAG	5655349–5655329
csgD$_F$ (promoter)	GATCAGATCTTGAAACCCCGCTTTTTTTATTG	1547424–1547445
csgD$_R$ (promoter)	GATCGTCGACAATGTACAACTTTTCTATCATTTC	1547694–1547671

[a] Nucleotide sequence of *E. coli* primers used in this study were selected from the published genome sequence of *E. coli* O157:H7 strain EDL933 with the accession number AE005174.2.
[b] Location refers to the position of primer sequence in the genome of EDL933.
[c] Subscripts F, R, and P indicate forward primers, reverse primers, and TaqMan probes; "RT-PCR" denotes primers used in reverse transcriptase-based quantitative PCR.

plate was incubated at 37°C or 30°C in an automated growth curve reader programmed for continuous shaking and collecting optical density readings at 600 nm (OD_{600}) every 30 min (Growth Curves USA, Piscataway, NJ). The optical density data were analyzed by using GraphPad Prism 6 software (GraphPad Software, Inc., La Jolla, CA). The generation times of bacterial strains were estimated from the exponential portions of the growth curves and equaled the time required for the doubling of the OD_{600}.

Recombinant DNA procedures. The construction of the *hha* deletion mutant and the *hha*-complementing plasmid (pSM197R) has been described previously (44). A previously reported recombineering method was used for deleting the *csgA* gene in the wild-type and *hha* mutant strains to construct the *csgA* and *hha csgA* deletion mutants, respectively (49). Briefly, a 1.2-kb fragment containing the neomycin resistance gene (*neo*), which was flanked at its 5′ and 3′ ends with 45 and 46 bases of *csgA* upstream and downstream nucleotide sequences, respectively, was generated by PCR using a FailSafe PCR kit (Epicenter, Madison, WI). The nucleotides sequences of 5′ and 3′ primers used in this PCR were **CGTG ACACAACGTTAATTTCCATTCGACTTTTAAATCAATCCGAT**AGC TGAATGAGTGACGTGC and **GTTACCAAAGCCAACCTGAGTTA CGTTGACGGTGGAATTAGATGCA**TAGAGCAGTGACGTAGT CGC, respectively. The nucleotides in bold type represent sequences complementary to the nucleotide sequences located immediately at the 5′ and 3′ ends, respectively, of the *csgA* gene. The underlined nucleotides represent nucleotides complementary to the 5′ and 3′ ends, respectively, of the oBBI 92/93 *neo* cassette containing FRT (flippase recognition target) sequences for enabling a FLP (flippase recombination enzyme)-catalyzed deletion of *neo* (50). The PCR fragment was gel purified and electroporated into the arabinose-induced competent cells of the wild-type and isogenic *hha* mutant strains of O157 containing the plasmid pKD46 (49). Kanamycin-resistant transformants were screened by PCR for the replacement of *csgA* with the *neo* gene. The kanamycin-resistant *csgA* deletion mutant (*csgA* mutant) was transformed with plasmid pCP20 encoding FLP recombinase (51) to facilitate deletion of the *neo* gene when the *csgA* mutant was grown at 37°C. For complementation of the *csgA* deletion mutation, the 1.5-kb DNA fragment containing the *csgBAC* operon was isolated by PCR using primers *csgBAC*$_F$ and *csgBAC*$_R$ (Table 2). The PCR-amplified DNA was resolved in a 1% agarose gel by a standard DNA gel electrophoresis technique, and the 1.5-kb DNA fragment was excised from the gel and purified with a gel extraction kit according to the manufacturer's recommended protocol (Qiagen Inc., Valencia, CA). The purified 1.5-kb fragment was cloned in pCR2.1 TOPO cloning system using *E. coli* TOP10 electrocompetent cells and the manufacturers' recommended protocol (Invitrogen, Carlsbad, CA). The pCR2.1 plasmid carrying *csgBAC* was named pSM569 (Table 1).

Quantitative reverse transcriptase PCR (QRT-PCR). Bacterial strains grown overnight with shaking (200 rpm) at 37°C in LB broth containing carbenicillin at 100 μg ml^{-1} (LB-Carb) were diluted 1:100 into fresh YESCA-Carb and incubated at 30°C or 37°C until the culture A_{600} was 1.3 to 1.4 (5 to 5.5 h). One milliliter of bacterial culture was mixed with 2 ml of RNA Protect solution and processed for RNA isolation using the RNeasy minikit (Qiagen Inc., Valencia, CA). RNA was treated with Turbo DNase for DNA removal (Applied Biosystems/Ambion, Austin, TX). QRT-PCR was performed by adding 50 ng of RNA, 0.75 μM (each) antisense and sense primers, 0.25 μM TaqMan probe (labeled at the 5′ and 3′ ends with FAM reporter and TAMRA quencher dyes, respectively) (Table 2) to QRT-PCR Master Mix (Agilent Technologies, Inc., Santa Clara, CA). The reaction mixtures were incubated in a Mx3005P (Agilent Technologies, Inc., Santa Clara, CA) for cDNA synthesis (50°C for 30 min), amplification, and real-time detection of amplified products (95°C for 10 min; 35 cycles of 95°C for 30 s, 55°C for 60 s, 72°C for 30 s) specific for *fliC*, *csgA*, *flhD*, and *csgD*. The expression of each of the four genes in the mutant strain was compared to the expression of the same genes in the wild type and the mutant strain complemented for the deleted gene using the Mx3005 software. The expression data were normalized to endogenous levels of *rpoA* in order to account for any minor variations in the amounts of RNA across samples. The expression data for each target gene in the mutant strains were plotted as relative expression by adjusting the expression of the same gene in the wild-type calibrator strain to 1.

Quantification of biofilm formation. The bacterial cultures grown overnight at 37°C with shaking (200 rpm) in YESCA-Carb were diluted 1:100 in fresh YESCA-Carb. To quantify total biofilm biomass, 200 μl of

the diluted culture was added into the wells of 96-well, round-bottom microtiter plates (Immulon, 2HB; Thermo Scientific, Milford, MA). Inoculating four independently grown cultures into 6 wells each resulted in a total of 24 wells being analyzed for the production of biofilms per strain. To determine the proportion of viable cells present in biofilms, 2 ml of 1:100 diluted overnight cultures prepared in YESCA-Carb from three independently grown cultures was added to 13-ml disposable plastic tubes with snap caps. After 48 h of incubation at 30°C or 37°C, the growth medium was aspirated, and plates or tubes were rinsed with phosphate-buffered saline (PBS, pH 7.3). The biofilms produced in the plates were heat fixed (30 min at 80°C), stained with 0.1% crystal violet for 30 min at 25°C, and washed three times with PBS. The wells were filled with 200 μl of 95% ethanol, and absorbance at 590 nm was measured to quantify the total biofilm mass (48). The biofilms produced in 13-ml tubes were not subjected to heat fixation and were scraped off into 1 ml of PBS with a sterile wooden applicator, vortexed vigorously, and diluted in 10-fold serial dilutions in PBS, and 100-μl aliquots of these dilutions were plated on LB agar containing carbenicillin (100 μg ml^{-1}). The agar plates were incubated at 37°C for 24 h, and bacterial colonies produced on these plates were enumerated.

Determination of Congo red binding by bacterial cells. Overnight cultures of bacterial strains grown in LB-Carb were streaked on Congo red agar plates. After incubation for 36 to 48 h at 30°C or 18 to 24 h at 37°C, plates were photographed.

Determination of bacterial motility. For swimming motility assays, overnight bacterial cultures grown in LB-Carb were centrifuged at 10,000 × *g* for 2 min to pellet bacterial cells. The cell pellets were resuspended in YESCA broth at one-tenth the original volume of the culture, and 2 μl of this suspension was spotted on motility plates (YESCA broth containing 0.33% Noble agar and carbenicillin at 100 μg ml^{-1}). The diameters of motility halos were determined after incubation for 24 to 36 h at 30°C and 12 to 16 h at 37°C.

Gel shift assays. For gel shift assays, DNA fragments containing promoter sequences for *flhDC* and *csgD* were amplified by PCR using primers (Table 2) and an AmpliTaq Gold DNA polymerase-containing kit according to the manufacturer's instructions (Life Technologies, Grand Island, NY). The PCR amplified fragments were resolved on 2% agarose gels by electrophoresis and extracted from the gel using a Qiagen gel extraction kit according to the manufacturer's recommended protocol (Qiagen Inc., Valencia, CA). Each gel-purified fragment (100 ng) was incubated in a 20-μl reaction volume containing excess of poly(dI-dC) and 2-fold-increasing amounts (0 to 4 μg) of Hha and a 1× reaction buffer (44). After 20 min at 25°C, the promoter-Hha mixtures were analyzed on a 6% nondenaturing polyacrylamide gel (44). The gel was stained for 20 min in Sybr green diluted to 1× per the instructions of the manufacturer (Molecular Probes). The stained gel was visualized using a charge-coupled device (CCD) camera equipped with a 510-nm filter to capture Sybr green fluorescence.

Statistics. Statistical analysis of the data for the biofilm production, motility zones, and gene expression was performed by using GraphPad Prism 6 (GraphPad Software, Inc., La Jolla, CA). The statistical significance of the differences in the sample means of the mutant and wild-type strain was calculated by using the unpaired Student's *t* test. Results were considered significant at a *P* value of <0.05.

RESULTS

The generation times of mutant bacterial strains were similar to those of the wild-type bacterial strain. Reduced bacterial growth in response to specific environmental and nutritional factors, such as suboptimal growth temperatures and limiting nutrients, and due to genetic aberrations has been linked to increased biofilm formation (23, 26, 27, 36). Although temperatures between 26°C and 30°C are considered conducive to biofilm formation, many *E. coli* and *E. coli* O157 strains are capable of producing biofilms at 37°C (9, 12, 40). Thus, in order to determine the molecular basis of

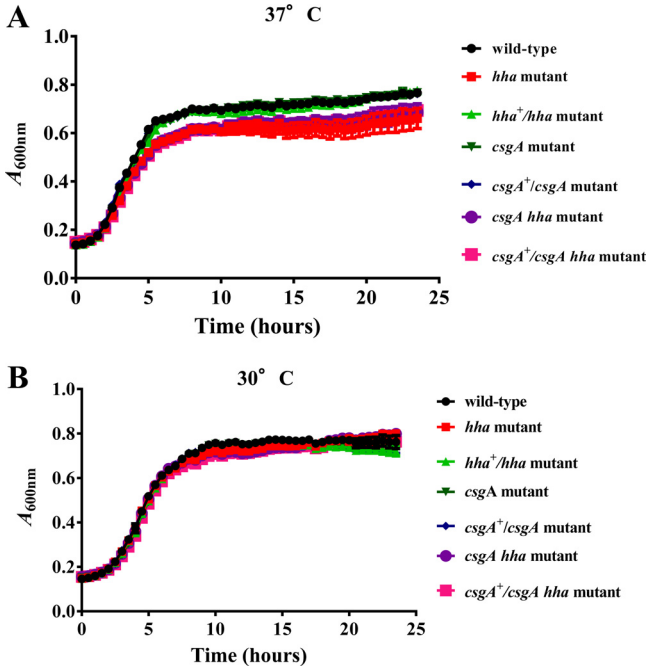

FIG 1 Determination of bacterial generation times at 37°C and 30°C in YESCA broth. Bacterial strains were grown for 24 h in YESCA broth, and optical density at 600 nm (OD_{600}) was recorded every 30 min. Three independent cultures were tested in triplicate, and each point on the growth curve represents an average of nine readings. The generation times were determined by computing the time required for doubling of the optical density of the bacterial culture during the exponential phase of growth.

hha regulation of biofilm formation at 37°C (body temperature of the human host) and 30°C, we first ascertained that wild-type O157 and its isogenic *hha*, *csgA*, and *hha csgA* mutants would have similar growth rates at 37°C and 30°C. For this, 1:100 dilutions of overnight (37°C) bacterial cultures were cultivated in YESCA-Carb at 37°C or 30°C for 24 h with continuous shaking in an automated growth reader. This instrument is suitable for analyzing growth kinetics of large numbers of bacterial strains and has excellent sensitivity to detect differences in bacterial growth kinetics. However, the major limitation of this growth analyzer is that the generation times computed from the growth curves produced by this system cannot be compared to the generation times calculated from growth curves resulting from bacterial growth in large-volume flasks subjected to vigorous shaking. In other words, the OD_{600} of bacterial cultures in the microtiter plate wells of the growth reader increases by much smaller increments than that of cultures grown in larger vessels with a several-times air-to-culture volume ratio. In addition, small culture volumes that are confined to the wells of a microtiter plate are not conducive to achieving the high cell densities that are easily attained in large-volume containers over a shorter time (data not shown). The main purpose, therefore, of using this instrument was to determine if there are substantial differences in the growth kinetics of the strains that we used in this study, and the data that we obtained clearly showed that the generation times for each of the seven bacterial strains were fairly similar to each other. The generation times at 37°C ranged from 82 to 97 min and were shorter than the generation times for these strains at 30°C (112 to 128 min) (Fig. 1). The generation times of bacterial strains carrying the *hha* deletion were

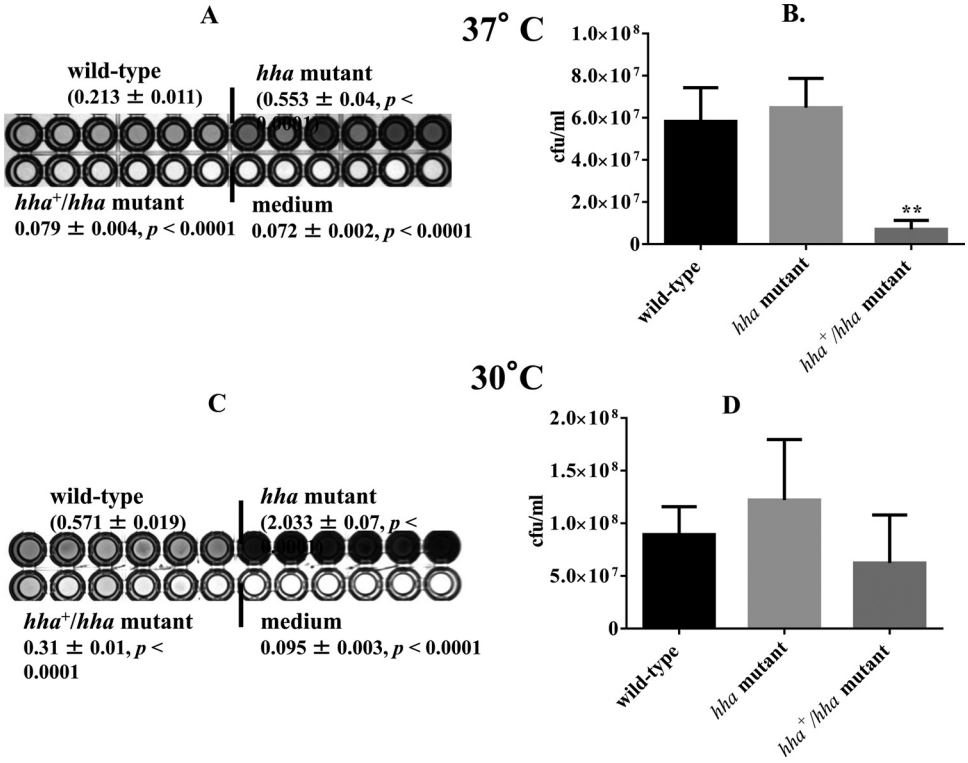

FIG 2 Effect of *hha* on the biofilm formation and on the proportion of viable bacterial cells recovered from biofilms at 37°C and 30°C after 48 h of growth in YESCA broth. Total biofilm masses produced by the wild type, *hha* mutant, and the *hha*-complemented mutant (*hha*$^+$/*hha* mutant) at 37°C (A) and 30°C (C) are given as averages ± standard errors of the means (SEM) for 24 replicate wells from four independent cultures. Only 6 of 24 wells are shown for each strain. Significant ($P < 0.05$) differences in biofilm biomass between the wild-type and the mutant were determined using an unpaired Student's *t* test (Mann-Whitney test). The proportion of viable bacterial cells recovered from biofilms are shown as bars representing average CFU ml^{-1} of three independent cultures of the wild-type, *hha* mutant, and *hha*$^+$/*hha* mutant grown at 37°C (B) and 30°C (D). Error bars represent the SEM. Significant differences between the wild-type and mutant strains were calculated as described above. **, $P < 0.005$.

slightly longer at both 37°C (97 min) and 30°C (128 min) than those of the *hha*-positive strains (Fig. 1).

Biofilm formation was enhanced and bacterial motility was reduced in *hha* mutant strains at 37°C and 30°C, but the expression of the flagellar gene *fliC* decreased only at 37°C. The total biofilm mass produced by the *hha* mutant was 2.5-fold higher ($P < 0.0001$) than that of the wild-type strain at 37°C, as indicated by the higher intensity of the blue color produced in the wells inoculated with the mutant strain (Fig. 2A). The mean intensity of the blue (0.079) color for the *hha* mutant complemented with a plasmid-cloned *hha* (pSM197R) was equivalent to that produced in the medium control wells, indicating that increased expression of *hha* from pSM197R (a multicopy plasmid) exerts a negative effect on biofilm formation (Fig. 2A). The proportions of viable cells recovered from the biofilms produced by the *hha* mutant were about 1.1-fold higher ($P = 0.305$) than those recovered from the biofilms produced by the wild-type strain (Fig. 2B). The numbers of viable bacterial cells in the biofilms produced by the *hha*-complemented strain (*hha*$^+$/*hha* mutant) were 8-fold ($P < 0.0022$) and 9.1-fold ($P < 0.0022$) lower than those of the wild-type and *hha* mutant strains, respectively (Fig. 2B). On the other hand, the largest amount of total biofilm mass was produced by the *hha* mutant after 48 h of growth at 30°C, as indicated by the development of the dark blue color in the wells inoculated with this strain (Fig. 2C). The biofilm mass produced by the *hha* mutant at 30°C was 3.5-fold and 6.5-fold ($P < 0.0001$) higher than those of the wild-type and *hha*$^+$/*hha* mutant strains, respectively (Fig. 2C). The *hha*$^+$/*hha* mutant was a faint shade of blue whose intensity was approximately 2-fold lower ($P < 0.0001$) than that of the wild-type strain (Fig. 2C). The numbers of viable cells recovered from the biofilms produced by the *hha* mutant at 30°C were about 1.4-fold higher ($P = 0.387$) than those recovered from the wild-type strain (Fig. 2D). The *hha*$^+$/*hha* mutant showed recovery of 0.7-fold ($P = 0.238$) and 2-fold ($P = 0.132$) fewer viable cells than the wild-type and *hha* mutant strains, respectively (Fig. 2D). The medium control wells appeared white.

Bacterial motility has also been shown to be an important factor in the transition from a planktonic state to a sedentary state, as a prerequisite for biofilm formation, and in segregation and dispersal of mature biofilms (15). Determination of the relative motility of bacterial strains on motility plates showed that the *hha* mutant produced much smaller motility zones than the wild-type strain, and the motility zones produced by the *hha*-complemented *hha*$^+$/*hha* strain were larger than those of the wild-type strain (Fig. 3A and C). Based on the measurements of the diameters of the motility zones produced at 37°C, motility zones of the *hha* mutant were 3.0-fold ($P = 0.0079$) smaller than that of the wild-type strain. The motility zones of the complemented *hha*$^+$/*hha* mutant were 1.2-fold larger than that of the wild-type strain, presumably due to the *hha* dosage effect from pSM197R (Fig. 3B). The complementation of the motility deficiency in the *hha* mutant by pSM197R confirmed that *hha* is a positive regulator of motility in

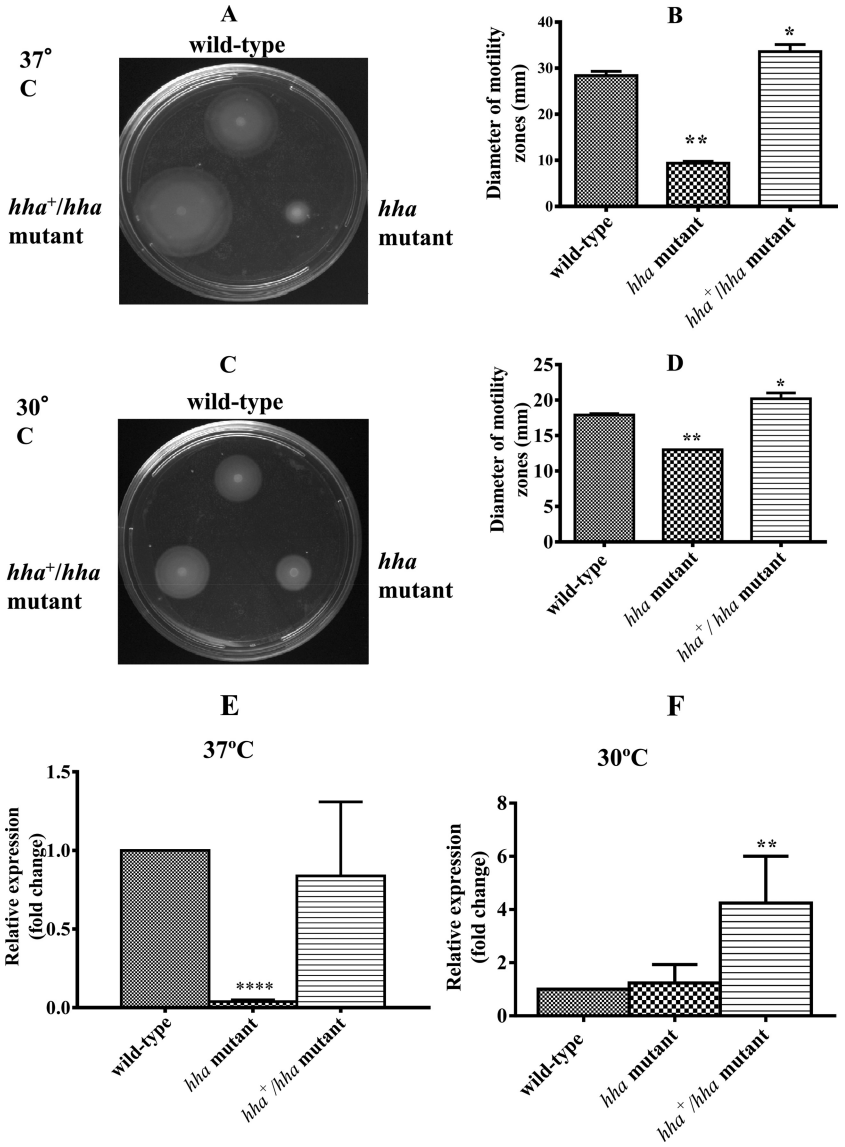

FIG 3 Effect of *hha* on bacterial motility and flagellar gene (*fliC*) expression at 37°C and 30°C. (A and C) The motility of wild-type, *hha* mutant, and *hha*$^+$/*hha* mutant strains was determined by spotting 10-fold-concentrated overnight bacterial cultures on 0.33% soft agar plates. The diameter of the motility zone produced around the point of bacterial inoculation was measured after incubation for 12 to 16 h at 37°C (A) or 24 to 36 h at 30°C (C). (B and D) Diameters of swimming or motility zones of five independent bacterial cultures grown overnight at 37°C (B) and 30°C (D). (E and F) The expression of *fliC* was determined by QRT-PCR, and DNA-free RNA was prepared from the wild-type, *hha* mutant, and *hha*$^+$/*hha* mutant strains grown at 37°C (E) and 30°C (F). Bars represent the average relative expression of *fliC* determined using RNA from three independent bacterial cultures. Error bars represent the SEM. Significant ($P < 0.05$) differences in motility between the wild-type and mutant strains were determined using an unpaired Student's *t* test (Mann-Whitney test). *, $P = 0.0317$; **, $P = 0.0079$. For *fliC* gene expression, significant ($P < 0.05$) differences between the wild-type and mutant strains were determined using an unpaired Student's *t* test and Welch's correction. **, $P = 0.0063$; ****, $P < 0.0001$.

O157 (41). The mean diameter of the motility zones produced at 30°C by the *hha* mutant was about 1.4-fold smaller ($P = 0.0079$) than that of zones produced by the wild-type strain (Fig. 3D). The motility zones produced by the complemented *hha*$^+$/*hha* mutant were about 1.1-fold ($P = 0.0317$) and 1.5-fold ($P = 0.0079$) larger in diameter than those of the wild-type and *hha* mutant strains, respectively (Fig. 3D).

Since increased biofilm formation correlated with reduced motility in the *hha* mutant strain at both 37°C and 30°C, and complementation of *hha* mutant with pSM197R restored its motility to the wild-type levels, we examined whether the expression of *fliC* was equally affected at 37°C and 30°C. The QRT-PCR analysis of RNA prepared from bacterial strains grown at 37°C showed a 26-fold ($P < 0.0001$) reduction in the *fliC* gene expression in the *hha* mutant compared to the wild-type strain (Fig. 3E). The complementation with pSM197R restored the expression of *fliC* in the *hha* mutant to the wild-type levels ($P = 0.611$) (Fig. 3E). The QRT-PCR analysis of bacterial strains grown at 30°C showed no significant difference in the *fliC* gene expression between the *hha* mutant and the wild-type strain ($P = 0.436$) (Fig. 3F). However, complementation with pSM197R increased *fliC* expression in the *hha* mutant strain 4-fold compared to expression in the wild-type

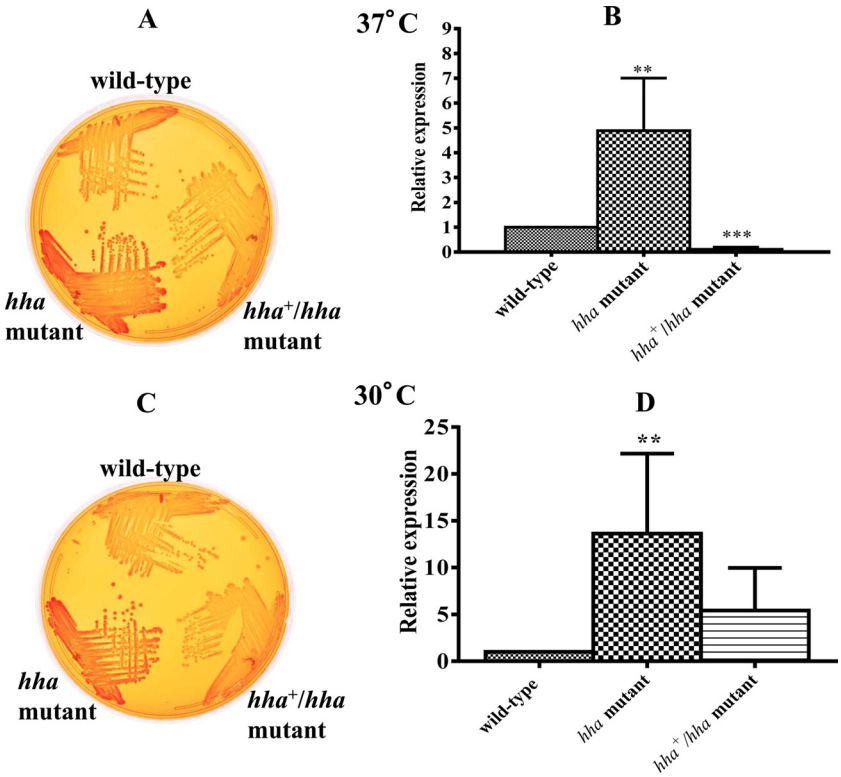

FIG 4 Correlation between Congo red binding by and curli gene (*csgA*) expression in the wild-type and *hha* mutant at 37°C and 30°C. Congo red binding was assessed based on the intensity of the red color of the colonies produced on YESCA agar containing Congo red after incubation for 24 h at 37°C (A) or after incubation for 48 h at 30°C (C). Coloration of the colonies was interpreted as light red (low), dark red (intermediate), or darker red (high). The expression of *csgA*, the gene encoding curlin of curli fimbriae, was determined by QRT-PCR using DNA-free RNA prepared from the wild-type, *hha* mutant, and *hha*$^+$/*hha* mutant strains grown at 37°C (B) and 30°C (D). Bars with different hatching patterns represent the average relative expression of *csgA* determined using RNA from three independent bacterial cultures grown at 37°C (B) and 30°C (D). Error bars represent the SEM. Significant ($P < 0.05$) differences between the wild-type and mutant strains were determined using an unpaired Student's *t* test and Welch's correction. **, $P = 0.004$; ***, $P < 0.0001$.

strain ($P = 0.0063$) (Fig. 3F). Thus, the presence of multiple copies of *hha* enhanced *fliC* expression at 37°C and 30°C.

Increased biofilm formation by the *hha* mutant resulted from increased expression of curli independent of growth temperature. Among the cell surface components, curli fimbriae play an important role in the formation of biofilms (8, 28). Although the temperature range of 26°C to 30°C is considered optimal for the expression of curli fibers (28), many commensal and pathogenic strains of *E. coli*, including O157:H7 and O157:NM serotypes, are capable of expressing and assembling curli fibers on their cell surfaces at 37°C (9, 12, 40). Phenotypic expression of curli fimbriae on bacterial cell surfaces can be inferred from the intensity of the red color of the colonies produced on Congo red indicator plates (47, 48). The bacterial colonies produced by the *hha* mutant were dark red following 24 h of growth at 37°C (Fig. 4A) or 48 h of growth at 30°C (Fig. 4C), compared to the light red colonies of the wild-type strain. The *hha* mutant complemented with pSM197R produced colonies that had slightly weaker red coloration than the wild-type strain at both temperatures, presumably due to the increased production of *hha* from pSM197R (Fig. 4A and C). Since Congo red binding provides a qualitative assessment of the expression of curli fimbriae at the bacterial cell surface, we next determined by QRT-PCR whether the increased Congo red binding by the *hha* mutant strain correlated with the increased expression of *csgA*, the gene encoding curlin of curli fimbriae. QRT-PCR analysis showed that in the *hha* mutant, the expression of *csgA* increased about 5-fold when the strain was grown at 37°C (Fig. 4B) and about 14-fold (Fig. 4D) ($P = 0.002$) when the strain was grown at 30°C, compared to expression in the wild-type strain. The complementation of the *hha* mutant with pSM197R caused significant reduction (about 8-fold) ($P = 0.0098$) in *csgA* expression in cultures grown at 37°C (Fig. 4B). In the *hha*$^+$/*hha* mutant grown at 30°C, the expression of *csgA* was reduced about 5-fold ($P = 0.0022$) compared to that in the *hha* mutant strain (Fig. 4D) but did not decrease completely to the wild-type level (Fig. 4D).

Curli fimbriae are important for biofilm formation in O157. Curli fimbriae are among the most important cell surface structures for biofilm formation in *E. coli*, and expression of curli fimbriae is turned on in the early stationary phase (8, 23). In order to assess whether the increased biofilm formation and Congo red binding by the *hha* mutant were due to the increased production of curli fimbriae, which are encoded by the *csgA* gene, we examined the effect of *csgA* deletion on production of biofilm and Congo red binding in the wild type and the *hha* mutant at 30°C (a temperature that promotes enhanced Congo red binding and biofilm formation). The total biofilm mass produced by the *csgA* mutant was 2.5-fold lower ($P < 0.0001$) than that produced by the wild-type strain, and the intensity of the blue color produced by this mutant in the plate wells was similar to that in the wells inoc-

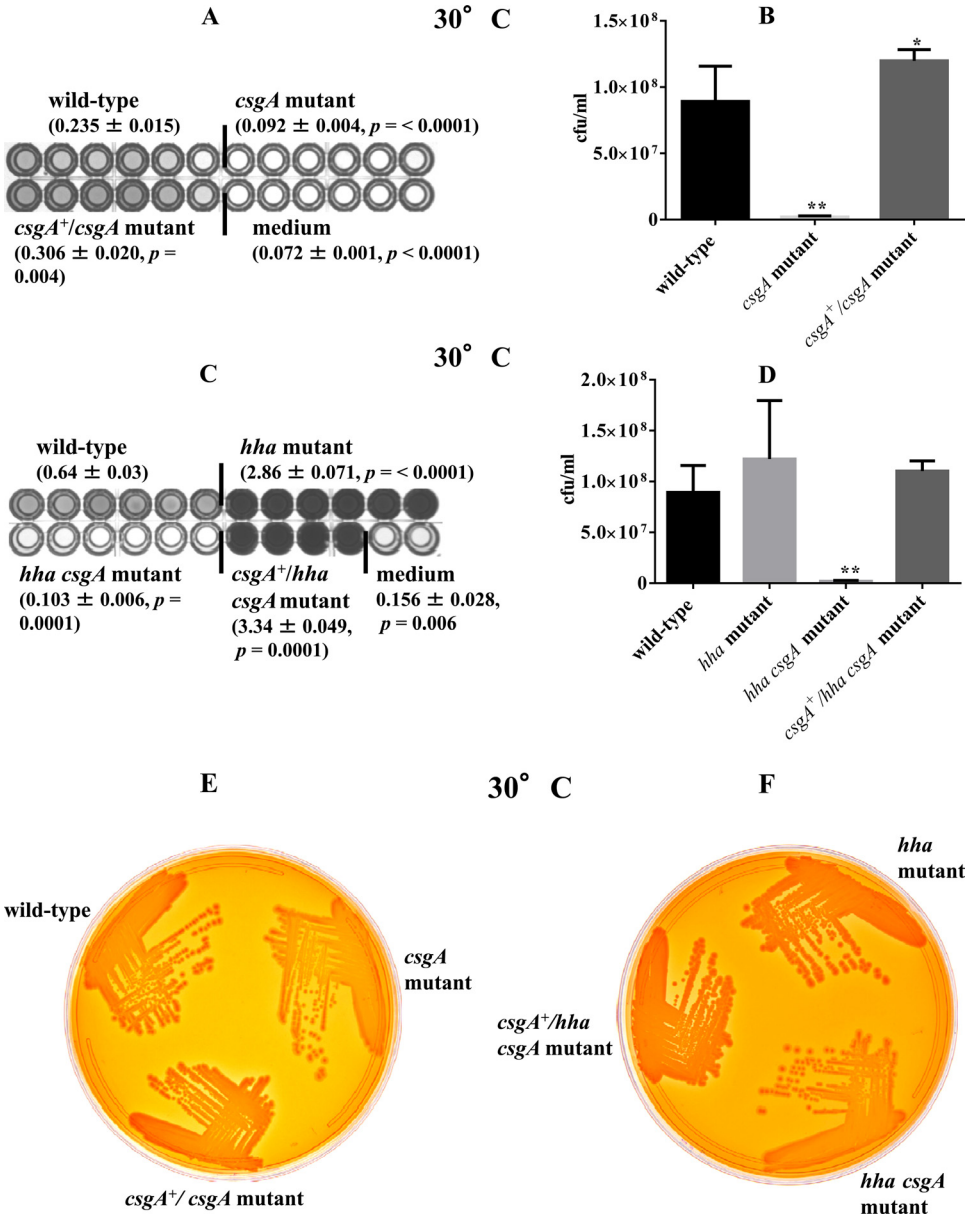

FIG 5 Requirement of *csgA* (A and B) and effect of *csgA* expression (C and D) on biofilm formation, recovery of viable bacterial cells from biofilms, and Congo red binding (E and F) after 48 h of growth at 30°C. Values for total biofilm mass produced are averages ± standard errors of the means (SEM) for 24 replicate wells (A) and 22 replicate wells (C) from four independent cultures. Only 6 of 24 wells are shown for the each strain, except for the *csgA*$^+$*/hha csgA* mutant strain, for which 4 of 22 wells are shown. Significant ($P < 0.05$) differences in biofilm biomass comparing the wild-type and mutant strains were determined using an unpaired Student's *t* test (Mann-Whitney test). (B and D) Numbers of viable bacterial cells recovered from biofilms, shown as average CFU ml^{-1} for three independent cultures of the wild-type, *csgA* mutant, and *csgA*-complemented (*csgA*$^+$*/csgA*) mutant (B) and wild-type, *hha* mutant, *hha csgA* mutant, and *csgA*-complemented (*csgA*$^+$*/hha csgA*) mutant (D). Error bars represent the SEM. Significant ($P < 0.05$) differences between the wild-type and mutant strains were determined using an unpaired Student's *t* test (Mann-Whitney). *, $P = 0.041$; **, $P = 0.0022$. (E and F) Congo red binding was assessed based on the intensity of the red color of the colonies produced on YESCA agar containing Congo red after incubation for 48 h at 30°C. Coloration of the colonies was interpreted as light red (low), dark red (intermediate), or darker red (high).

ulated with YESCA broth (medium control), indicating that the *csgA* deletion compromises the ability of *csgA* mutant to produce biofilms (Fig. 5A). The ability of the *csgA* mutant to produce biofilm was restored to wild-type levels by complementation with a plasmid-cloned *csgA* (pSM569) (Fig. 5A). The *csgA* mutant also showed significantly lower recovery of viable cells from the biofilms (1.90×10^6 CFU ml^{-1}; $P = 0.0022$) than the wild-type strain (8.9×10^7 CFU ml^{-1}) (Fig. 5B). The complementation of the *csgA* mutant with pSM569 resulted in recovery of viable cells (1.19×10^8, $P = 0.041$) that was only slightly but significantly higher than that in the wild-type strain (8.9×10^7 CFU ml^{-1}), indicating a gene-dosage effect of pSM569 (Fig. 5B). Since the *hha* mutant produced higher levels of biofilm than the wild-type strain, we also determined whether *csgA* deletion would abolish the biofilm formation in the *hha* mutant. The *hha* mutant produced total biofilm mass that was 4.5-fold higher ($P < 0.0001$) than that produced by

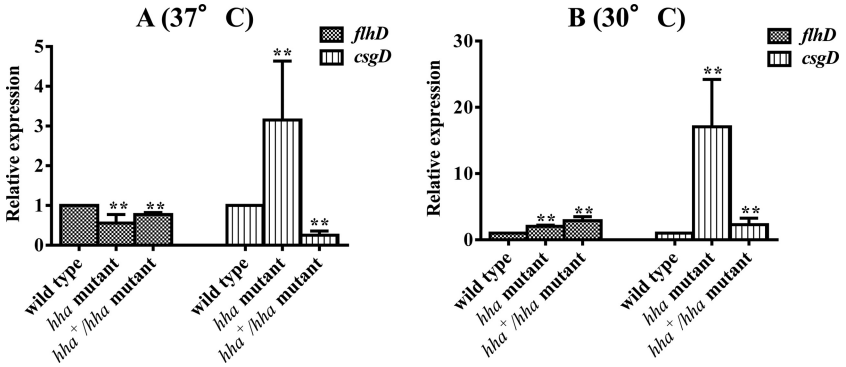

FIG 6 Differential effects of *hha* on *flhD* and *csgD* expression. DNA-free RNAs were subjected to real-time QRT-PCR. Relative transcriptional levels of *flhD* and *csgD* were determined by QRT-PCR and DNA-free RNA prepared from three independent bacterial cultures of the wild-type, *hha* mutant, and *hha*$^+$/*hha* mutant at 37°C (A) and 30°C (B). Relative expressions of *flhD* and *csgD* were normalized to the transcriptional levels of the *rpoA* gene. Values are expression of *flhD* and *csgD* in the mutant and complemented mutant strains relative to the expression of these genes in the wild-type strain. Error bars represent the SEM. Significant ($P < 0.05$) differences between the wild-type and mutant strains were determined using an unpaired Student's *t* test (Mann-Whitney). **, $P = 0.0022$.

the wild-type strain, but the biofilm mass produced by the *hha csgA* mutant was reduced 22-fold compared to that of the *hha* mutant and 6-fold compared to that of the wild-type strain (Fig. 5C). The complementation of the *hha csgA* mutant strain by pSM569 increased its biofilm mass production to levels that were about 1.2-fold higher than those of the *hha* mutant (Fig. 5C). These effects of *csgA* and *hha* on biofilm production correlated with the proportions of viable bacterial cells recovered from the biofilms. As shown in Fig. 5D, the *hha csgA* mutant had 65-fold and 48-fold fewer viable cells (1.85×10^6 CFU ml^{-1}; $P = 0.0022$) recovered from its biofilms than the *hha* mutant (1.22×10^8 CFU ml^{-1}) and wild-type strain (8.9×10^7 CFU ml^{-1}), respectively. The complementation of *hha csgA* mutant with pSM569 restored the level of viable bacterial cells in its biofilms (1.1×10^8 CFU ml^{-1}) to levels similar to those recovered from the wild type (8.9×10^7 CFU ml^{-1}) and the *hha* mutant strain (1.22×10^8 CFU ml^{-1}) (Fig. 5D). These results indicated that *csgA* is the key gene conferring on O157 the ability to produce biofilms and that Hha is the negative regulator of *csgA* expression.

The effects of the differential expression of *csgA* on the formation of biofilms in the wild-type, *hha*, and *hha csgA* strains with or without complementation for *csgA* were also assessed in terms of the degree of Congo red binding. The *csgA* mutant produced lighter red colonies on Congo red plates after 48 h of incubation at 30°C, in contrast to the dark red colonies of the wild type and the *csgA* mutant complemented with pSM569 (Fig. 5E). The *hha* mutant produced darker red colonies in the presence of the *csgA* gene, because the colonies produced by the *hha csgA* mutant on the Congo red medium were a lighter red (Fig. 5F). The complementation of *hha csgA* mutant with pSM569 restored a dark-red colony phenotype (Fig. 5F). The results of the Congo red binding assay corroborated the data generated by quantitative biofilm and QRT-PCR assays and demonstrated that *hha* regulates biofilm formation in O157 by the negative regulation of *csgA*.

Reduced motility and increased Congo red binding correlated with reduced *flhD* and increased *csgD* transcriptional levels. We showed previously that *hha* deletion resulted in reduced motility and enhanced curli expression due to reduced *fliC* and increased *csgA* transcriptional levels, respectively (41). Since global regulators FlhDC and CsgD control *fliC* and *csgA* expression, respectively (21, 23, 24), we examined if transcriptional levels of *flhD* and *csgD* would correlate with the transcriptional levels of *fliC* and *csgA* in the *hha* mutant strain. The transcriptional analysis showed that the *flhD* level was reduced about 2-fold in the *hha* mutant strain, and complementation of this mutant with pSM197R restored *flhD* expression similar to that in the wild-type strain at 37°C (Fig. 6A). On the other hand, expression of *csgD* was increased 3-fold in the *hha* mutant strain, while the expression of *csgD* was reduced 4-fold in the *hha* mutant complemented with pSM197R compared to that in the wild-type strain at 37°C (Fig. 6A). At 30°C, however, the expression of *flhD* was 2-fold and 3-fold higher in the *hha* and the *hha*$^+$/*hha* mutant strains, respectively (Fig. 6B). The expression of *csgD* at 30°C was 17-fold higher in the *hha* mutant than in the wild-type strain, but the complementation of *hha* mutant with pSM197R reduced the expression of *csgD* from 17-fold to only 2.3-fold higher than the wild-type strain.

Purified Hha binds to *flhDC* and *csgD* promoters in gel shift assays. Differential expression of *fliC* and *csgA* genes is essential for *E. coli* to switch from the planktonic to the sedentary life style in response to environmental cues (24). Because the expression of flagellar and curli genes is controlled by master regulators FlhDC and CsgD, and the expression of *flhD* and *csgD* was differentially affected in the *hha* mutant, especially at 37°C, we examined whether a purified Hha would bind to the promoter regions of *flhDC* and *csgDEFG* operons encoding the master regulators FlhDC and CsgD, which regulate transcription of *fliC* and *csgA* genes, respectively. Incubation of PCR-amplified fragments containing the promoter regions for *flhDC* (Fig. 7A) and *csgD* (Fig. 7B) with increasing concentrations of Hha and in the presence of a 10-fold molar excess of nonspecific competing DNA poly(dI-dC) showed reduction in the mobility of these fragments in a concentration-dependent manner relative to the same fragments incubated in the absence of Hha. The maximal shift in the mobility of the two promoter fragments was achieved at Hha concentrations of 2 to 4 μg (Fig. 7). These results indicated that Hha presumably regulates both *flhD* and *csgD* expression by its direct interactions with the *flhDC* and *csgDEFG* promoter regions in bacterial cells.

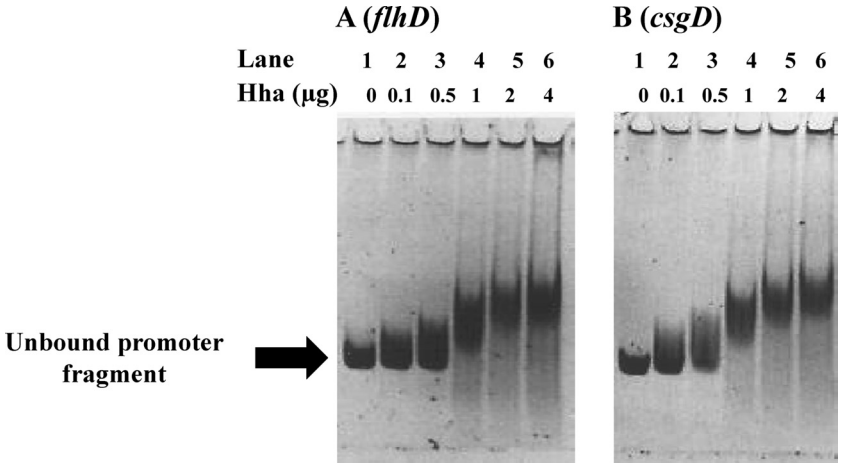

FIG 7 Gel shift assays for assessing the binding of Hha with promoter regions controlling transcription of *flhDC* and *csgD*. One hundred nanograms of PCR-amplified and gel-purified DNA fragments containing promoter regions for *flhDC* (A) and *csgD* (B) were incubated in a binding buffer with or without purified Hha protein for 20 min at room temperature. The samples were analyzed on a 6% nondenaturing polyacrylamide gel stained with SYBR green and visualized using a filter with a bandwidth of 520 nm. The promoter fragments were incubated with 0 μg (lane 1), 0.1 μg (lane 2), 0.5 μg (lane 3), 1 μg (lane 4), 2 μg (lane 5), and 4 μg (lane 6) of Hha. The arrow indicates the unbound *flhDC* and *csgDEFG* promoter fragments.

DISCUSSION

E. coli biofilms are complex sedentary communities, and their morphogenesis is highly coordinated and is controlled by several genetic factors and environmental and nutritional cues (3, 7, 15, 21, 23–25, 27, 52, 53). A critical step in transitioning from a planktonic state to biofilm formation is cessation or reduction in the expression of the flagellar system in order to reduce bacterial motility and promote expression of adhesive fimbriae, such as curli fimbriae, and other extracellular adhesins that allow adherence of bacterial cells to solid surfaces (8, 23). In the current study, we have demonstrated that Hha represses biofilm formation in O157 by induction of flagellar and repression of curli gene expression. In comparison to the wild-type and *hha*$^+$/*hha* mutant strains, the *hha* mutant showed significant reduction in bacterial motility but enhanced binding of Congo red, the phenotype indicative of increased curli production at both 37°C and 30°C (47, 48). The differentially affected motility and curli phenotypes in the *hha* mutant were restored to wild-type levels by complementation with pSM197R, indicating that Hha is responsible for regulating the expression of these two phenotypes. The transcriptional analysis revealed that *csgA* was expressed at significantly higher levels in the *hha* mutant than in the wild-type and *hha*$^+$/*hha* mutant strains at both 37°C and 30°C. The repressor effects of Hha that we observed with respect to curli gene expression have also been reported for several other bacterial virulence genes (42, 44, 54, 55). For example, Hha, a member of the Hha-YmoA family of small transcriptional regulatory proteins, was initially identified as a repressor of α-hemolysin expression in *E. coli* (42). Other virulence factors that are negatively regulated by Hha include genes required for adherence of pathogenic *E. coli* O157:H7 and *Salmonella* strains to animal tissues and tissue culture cells (44, 54). A recent study showed that Hha acts as a repressor of biofilm formation in nonpathogenic *E. coli* K-12 strains through the repression of type I fimbriae (56). Although type I fimbriae are not expressed by *E. coli* O157:H7 due to the locked-on promoter configuration of this operon (57), the negative effect of Hha on biofilm formation by the repression of curli genes in O157 suggests a broader role for Hha in regulation of different clusters of fimbrial genes and in the complex regulatory scheme controlling the transition from planktonic to biofilm formation.

Several studies have reported that production of flagella and curli fimbriae promotes adherence to and colonization of epithelial cells in animal models and tissue cultures (13, 40, 58, 59). Flagella, for example, are essential for bacterial motility and for maintaining bacterial cells in a planktonic state when conditions are favorable for rapid growth (60, 61). On the other hand, curli expression is increased under conditions that are less favorable for rapid growth but conducive to adherence to solid surfaces (8, 23). Low temperature is conducive to biofilm formation in environmental and pathogenic *E. coli* strains (8, 62). Our quantitative analysis of biofilm formation showed that the *hha* mutant produced significantly larger amounts of biofilm and contained higher counts of viable bacterial cells in biofilms than the wild-type and *hha*$^+$/*hha* mutant strains at both 37°C and 30°C. Overall, the *hha* mutant produced the largest amount of biofilm at 30°C compared to that at 37°C, and these results were in agreement with studies showing that low temperatures are conducive to biofilm formation in environmental and pathogenic *E. coli* strains (8, 62). Although the *hha* mutant produced larger amounts of biofilm than the wild-type strain at 37°C, these amounts were much lower than the amount of biofilm produced at 30°C. The differences in the amounts of biofilms produced at these two temperatures correlated with the highest transcriptional levels of *csgA* and *csgD* in the *hha* mutant grown at 30°C, in contrast those obtained at 37°C. The importance of *csgA* in biofilm formation, as has been shown by other studies (8, 63–66), was confirmed by demonstrating the inability of the *csgA* and *hha csgA* mutants to produce biofilms.

Since growth rates of wild-type and isogenic *hha* and *hha*$^+$/*hha* mutant strains were higher at 37°C than at 30°C, the lower level of biofilm production by the *hha* mutant at 37°C compared to at 30°C might in part be due to differences in growth physiology at these two temperatures. For example, it is conceivable that higher growth of the *hha* mutant strains at 37°C would prevent *csgD* expression from reaching levels that were expressed at 30°C. Since

increased expression of CsgD is critical for increased expression of *csgA* and biofilm formation (67), lower levels of CsgD would reduce biofilm production at 37°C compared to that at 30°C. It has also been shown that at growth temperatures of <32°C, *E. coli* exhibits a global-stress response resulting in upregulation of many RpoS-dependent regulons, including those that are involved in biofilm formation (30). A recent study has demonstrated that the production of indole, which inhibits biofilm formation, is enhanced when cultures are shifted from 30°C to 37°C (68).

Contrary to the enhanced expression of curli as indicated by the increased Congo red binding and biofilm formation, motility of *hha* mutant was significantly reduced at 37°C and 30°C. Although the motility halos produced by the *hha* and *hha*$^+$/*hha* mutants at 37°C were much bigger (presumably due to rapid cellular metabolism) than those produced at 30°C, the motility of *hha* mutant was reduced at both temperatures relative to the motilities of the wild-type and *hha*$^+$/*hha* mutant strains, though the reduction was more pronounced at 37°C than at 30°C. These results implied that a reduction in bacterial motility is essential for increased biofilm formation by the *hha* mutant strains. This reciprocal correlation between reduced motility or lack of motility and increased curli formation resulting in increased biofilm formation has been observed in the nonmotile O157 strains isolated from HUS patients (40). Although motility and transcriptional levels of *flhD* and *fliC* in the *hha* mutant strain were reduced at 37°C and reduced motility of the *hha* mutant was restored to levels even higher than those of the wild-type strain at 37°C and 30°C, the transcriptional levels of *fliC* were almost similar to and that of the *flhD* strain about 2-fold higher than that of the wild-type strain at 30°C. The latter results are not surprising given that the motility differences between the *hha* mutant and the wild-type strain were much less substantial at 30°C, and the reduced motility of *hha* mutant at 30°C could potentially be due either to the high levels of curli expression promoting bacterial aggregation and biofilm formation without affecting flagellar gene expression or to compromised flagellar motor functions (15, 17).

In vitro gel shift analysis revealed positive interactions of Hha with the promoter sequences of *flhDC* and *csgDEFG*, suggesting that similar interactions *in vivo*, which could be direct or indirect, regulate the expression of FlhDC and CsgD, two global regulators affecting the expression of not only the flagellar and curli gene regulons, respectively, but also many other regulons reported to directly or indirectly influence motility and biofilm formation in O157. Several factors, including bacterial growth rate, temperature, osmolarity, oxygen tension, and physiological stress due to nutrient limitation, affect relative expression of FlhDC and CsgD (23, 24, 53). Hence, diverse signal transduction mechanisms presumably work in a specific hierarchical order to respond to physical and physiological alterations in bacterial growth environments to affect and fine tune the expression of *flhDC* and *csgD* (36, 69–73). FlhDC and CsgD are considered to have hierarchical superiority in terms of their importance in regulation of bacterial motility and curli expression, respectively (21, 24). For example, FlhDC expression is regulated during the exponential and early post-exponential growth phases, while CsgD levels become higher during the stationary growth phase (24). In addition to FlhDC, which activate class II and class III flagellar and chemotaxis genes, several other transcriptional factors activate flagellar gene expression mostly by affecting the expression of *flhDC* (24, 52, 74). Similarly, expression of *csgD* is regulated by multiple transcriptional regulators (23, 24, 28, 75, 76). Based on the present study, which demonstrates Hha-mediated differential regulation of *flhDC* and *csgD*, and several other studies describing the negative regulation by Hha of many virulence-associated genes and regulons (41, 42, 44, 54), Hha could also qualify as a global regulator having a hierarchical superiority in the overall network of transcriptional regulators controlling bacterial motility, biofilm formation, and virulence gene expression.

ACKNOWLEDGMENTS

We thank Lindsay Smith, Robert Morgan, and Kellie Winter for technical assistance. We also thank Shawn Bearson and Randy Sacco for the critical review of the manuscript.

Mention of trade names or commercial products in this article is solely for the purpose of providing specific information and does not imply recommendation or endorsement by the U.S. Department of Agriculture.

REFERENCES

1. **Karmali MA.** 2004. Infection by Shiga toxin-producing *Escherichia coli*: an overview. Mol. Biotechnol. **26**:117–122.
2. **Nataro JP, Kaper JB.** 1998. Diarrheagenic *Escherichia coli.* Clin. Microbiol. Rev. **11**:142–201.
3. **O'Toole G, Kaplan HB, Kolter R.** 2000. Biofilm formation as microbial development. Annu. Rev. Microbiol. **54**:49–79.
4. **Saldana Z, Erdem AL, Schuller S, Okeke IN, Lucas M, Sivananthan A, Phillips AD, Kaper JB, Puente JL, Giron JA.** 2009. The *Escherichia coli* common pilus and the bundle-forming pilus act in concert during the formation of localized adherence by enteropathogenic *E. coli.* J. Bacteriol. **191**:3451–3461.
5. **Torres AG, Jeter C, Langley W, Matthysse AG.** 2005. Differential binding of *Escherichia coli* O157:H7 to alfalfa, human epithelial cells, and plastic is mediated by a variety of surface structures. Appl. Environ. Microbiol. **71**:8008–8015.
6. **Elliott SJ, Yu J, Kaper JB.** 1999. The cloned locus of enterocyte effacement from enterohemorrhagic *Escherichia coli* O157:H7 is unable to confer the attaching and effacing phenotype upon *E. coli* K-12. Infect. Immun. **67**:4260–4263.
7. **Costerton JW, Lewandowski Z, Caldwell DE, Korber DR, Lappin-Scott HM.** 1995. Microbial biofilms. Annu. Rev. Microbiol. **49**:711–745.
8. **Olsen A, Jonsson A, Normark S.** 1989. Fibronectin binding mediated by a novel class of surface organelles on *Escherichia coli.* Nature **338**:652–655.
9. **Bian Z, Brauner A, Li Y, Normark S.** 2000. Expression of and cytokine activation by *Escherichia coli* curli fibers in human sepsis. J. Infect. Dis. **181**:602–612.
10. **La Ragione RM, Collighan RJ, Woodward MJ.** 1999. Non-curliation of *Escherichia coli* O78:K80 isolates associated with IS1 insertion in *csgB* and reduced persistence in poultry infection. FEMS Microbiol. Lett. **175**:247–253.
11. **Olsen A, Wick MJ, Morgelin M, Bjorck L.** 1998. Curli, fibrous surface proteins of *Escherichia coli*, interact with major histocompatibility complex class I molecules. Infect. Immun. **66**:944–949.
12. **Saldana Z, Xicohtencatl-Cortes J, Avelino F, Phillips AD, Kaper JB, Puente JL, Giron JA.** 2009. Synergistic role of curli and cellulose in cell adherence and biofilm formation of attaching and effacing *Escherichia coli* and identification of Fis as a negative regulator of curli. Environ. Microbiol. **11**:992–1006.
13. **Uhlich GA, Keen JE, Elder RO.** 2002. Variations in the *csgD* promoter of *Escherichia coli* O157:H7 associated with increased virulence in mice and increased invasion of HEp-2 cells. Infect. Immun. **70**:395–399.
14. **Hammar M, Arnqvist A, Bian Z, Olsen A, Normark S.** 1995. Expression of two *csg* operons is required for production of fibronectin- and Congo red-binding curli polymers in *Escherichia coli* K-12. Mol. Microbiol. **18**:661–670.
15. **Pratt LA, Kolter R.** 1998. Genetic analysis of *Escherichia coli* biofilm formation: roles of flagella, motility, chemotaxis and type I pili. Mol. Microbiol. **30**:285–293.
16. **Sheikh J, Hicks S, Dall'Agnol M, Phillips AD, Nataro JP.** 2001. Roles for Fis and YafK in biofilm formation by enteroaggregative *Escherichia coli.* Mol. Microbiol. **41**:983–997.
17. **Barrios AF, Zuo R, Ren D, Wood TK.** 2006. Hha, YbaJ, and OmpA

regulate *Escherichia coli* K-12 biofilm formation and conjugation plasmids abolish motility. Biotechnol. Bioeng. **93**:188–200.
18. **Reisner A, Haagensen JA, Schembri MA, Zechner EL, Molin S.** 2003. Development and maturation of *Escherichia coli* K-12 biofilms. Mol. Microbiol. **48**:933–946.
19. **Gualdi L, Tagliabue L, Landini P.** 2007. Biofilm formation-gene expression relay system in *Escherichia coli*: modulation of σ^S-dependent gene expression by the CsgD regulatory protein via σ^S protein stabilization. J. Bacteriol. **189**:8034–8043.
20. **Claret L, Hughes C.** 2002. Interaction of the atypical prokaryotic transcription activator FlhD2C2 with early promoters of the flagellar gene hierarchy. J. Mol. Biol. **321**:185–199.
21. **Liu X, Matsumura P.** 1994. The FlhD/FlhC complex, a transcriptional activator of the *Escherichia coli* flagellar class II operons. J. Bacteriol. **176**: 7345–7351.
22. **Wang S, Fleming RT, Westbrook EM, Matsumura P, McKay DB.** 2006. Structure of the *Escherichia coli* FlhDC complex, a prokaryotic heteromeric regulator of transcription. J. Mol. Biol. **355**:798–808.
23. **Barnhart MM, Chapman MR.** 2006. Curli biogenesis and function. Annu. Rev. Microbiol. **60**:131–147.
24. **Pesavento C, Becker G, Sommerfeldt N, Possling A, Tschowri N, Mehlis A, Hengge R.** 2008. Inverse regulatory coordination of motility and curli-mediated adhesion in *Escherichia coli.* Genes Dev. **22**:2434–2446.
25. **Pruss BM, Besemann C, Denton A, Wolfe AJ.** 2006. A complex transcription network controls the early stages of biofilm development by *Escherichia coli.* J. Bacteriol. **188**:3731–3739.
26. **Barnhart MM, Lynem J, Chapman MR.** 2006. GlcNAc-6P levels modulate the expression of curli fibers by *Escherichia coli.* J. Bacteriol. **188**:5212–5219.
27. **Jubelin G, Vianney A, Beloin C, Ghigo JM, Lazzaroni JC, Lejeune P, Dorel C.** 2005. CpxR/OmpR interplay regulates curli gene expression in response to osmolarity in *Escherichia coli.* J. Bacteriol. **187**:2038–2049.
28. **Olsen A, Arnqvist A, Hammar M, Normark S.** 1993. Environmental regulation of curli production in *Escherichia coli.* Infect. Agents Dis. **2**:272–274.
29. **White-Ziegler CA, Malhowski AJ, Young S.** 2007. Human body temperature (37°C) increases the expression of iron, carbohydrate, and amino acid utilization genes in *Escherichia coli* K-12. J. Bacteriol. **189**:5429–5440.
30. **White-Ziegler CA, Um S, Perez NM, Berns AL, Malhowski AJ, Young S.** 2008. Low temperature (23°C) increases expression of biofilm-, cold-shock- and RpoS-dependent genes in *Escherichia coli* K-12. Microbiology **154**:148–166.
31. **Beloin C, Valle J, Latour-Lambert P, Faure P, Kzreminski M, Balestrino D, Haagensen JA, Molin S, Prensier G, Arbeille B, Ghigo JM.** 2004. Global impact of mature biofilm lifestyle on *Escherichia coli* K-12 gene expression. Mol. Microbiol. **51**:659–674.
32. **Domka J, Lee J, Bansal T, Wood TK.** 2007. Temporal gene-expression in *Escherichia coli* K-12 biofilms. Environ. Microbiol. **9**:332–346.
33. **Gadgil M, Kapur V, Hu WS.** 2005. Transcriptional response of *Escherichia coli* to temperature shift. Biotechnol. Prog. **21**:689–699.
34. **Ren D, Bedzyk LA, Thomas SM, Ye RW, Wood TK.** 2004. Gene expression in *Escherichia coli* biofilms. Appl. Microbiol. Biotechnol. **64**: 515–524.
35. **Wang X, Preston JF, III, Romeo T.** 2004. The *pgaABCD* locus of *Escherichia coli* promotes the synthesis of a polysaccharide adhesin required for biofilm formation. J. Bacteriol. **186**:2724–2734.
36. **Otto K, Silhavy TJ.** 2002. Surface sensing and adhesion of *Escherichia coli* controlled by the Cpx-signaling pathway. Proc. Natl. Acad. Sci. U. S. A. **99**:2287–2292.
37. **Konkel ME, Tilly K.** 2000. Temperature-regulated expression of bacterial virulence genes. Microbes Infect. **2**:157–166.
38. **Cassels FJ, Wolf MK.** 1995. Colonization factors of diarrheagenic *E. coli* and their intestinal receptors. J. Ind. Microbiol. **15**:214–226.
39. **Kumar CG, Anand SK.** 1998. Significance of microbial biofilms in food industry: a review. Int. J. Food Microbiol. **42**:9–27.
40. **Rosser T, Dransfield T, Allison L, Hanson M, Holden N, Evans J, Naylor S, La Ragione R, Low JC, Gally DL.** 2008. Pathogenic potential of emergent sorbitol-fermenting *Escherichia coli* O157:NM. Infect. Immun. **76**:5598–5607.
41. **Sharma VK, Bearson SM, Bearson BL.** 2010. Evaluation of the effects of *sdiA*, a *luxR* homologue, on adherence and motility of *Escherichia coli* O157:H7. Microbiology **156**:1303–1312.
42. **Nieto JM, Carmona M, Bolland S, Jubete Y, de la Cruz F, Juarez A.** 1991. The *hha* gene modulates haemolysin expression in *Escherichia coli.* Mol. Microbiol. **5**:1285–1293.
43. **Sharma VK, Carlson SA, Casey TA.** 2005. Hyperadherence of an *hha* mutant of *Escherichia coli* O157:H7 is correlated with enhanced expression of LEE-encoded adherence genes. FEMS Microbiol. Lett. **243**:189–196.
44. **Sharma VK, Zuerner RL.** 2004. Role of *hha* and *ler* in transcriptional regulation of the *esp* operon of enterohemorrhagic *Escherichia coli* O157: H7. J. Bacteriol. **186**:7290–7301.
45. Reference deleted.
46. **Griffin PM, Ostroff SM, Tauxe RV, Greene KD, Wells JG, Lewis JH, Blake PA.** 1988. Illnesses associated with *Escherichia coli* O157:H7 infections. A broad clinical spectrum. Ann. Intern. Med. **109**:705–712.
47. **Hammar M, Bian Z, Normark S.** 1996. Nucleator-dependent intercellular assembly of adhesive curli organelles in *Escherichia coli.* Proc. Natl. Acad. Sci. U. S. A. **93**:6562–6566.
48. **Uhlich GA, Cooke PH, Solomon EB.** 2006. Analyses of the red-dry-rough phenotype of an *Escherichia coli* O157:H7 strain and its role in biofilm formation and resistance to antibacterial agents. Appl. Environ. Microbiol. **72**:2564–2572.
49. **Datsenko KA, Wanner BL.** 2000. One-step inactivation of chromosomal genes in *Escherichia coli* K-12 using PCR products. Proc. Natl. Acad. Sci. U. S. A. **97**:6640–6645.
50. **Bearson BL, Bearson SM, Uthe JJ, Dowd SE, Houghton JO, Lee I, Toscano MJ, Lay DC, Jr.** 2008. Iron regulated genes of *Salmonella enterica* serovar Typhimurium in response to norepinephrine and the requirement of *fepDGC* for norepinephrine-enhanced growth. Microbes Infect. **10**: 807–816.
51. **Cherepanov PP, Wackernagel W.** 1995. Gene disruption in *Escherichia coli*: Tc^R and Km^R cassettes with the option of Flp-catalyzed excision of the antibiotic-resistance determinant. Gene **158**:9–14.
52. **Chilcott GS, Hughes KT.** 2000. Coupling of flagellar gene expression to flagellar assembly in *Salmonella enterica* serovar Typhimurium and *Escherichia coli.* Microbiol. Mol. Biol. Rev. **64**:694–708.
53. **Hengge-Aronis R.** 1999. Interplay of global regulators and cell physiology in the general stress response of *Escherichia coli.* Curr. Opin. Microbiol. **2**:148–152.
54. **Fahlen TF, Wilson RL, Boddicker JD, Jones BD.** 2001. Hha is a negative modulator of transcription of *hilA*, the *Salmonella enterica* serovar Typhimurium invasion gene transcriptional activator. J. Bacteriol. **183**:6620–6629.
55. **Mourino M, Madrid C, Balsalobre C, Prenafeta A, Munoa F, Blanco J, Blanco M, Blanco JE, Juarez A.** 1996. The Hha protein as a modulator of expression of virulence factors in *Escherichia coli.* Infect. Immun. **64**:2881–2884.
56. **Garcia-Contreras R, Zhang XS, Kim Y, Wood TK.** 2008. Protein translation and cell death: the role of rare tRNAs in biofilm formation and in activating dormant phage killer genes. PLoS One **3**:e2394. doi:10.1371/journal.pone.0002394.
57. **Roe AJ, Currie C, Smith DG, Gally DL.** 2001. Analysis of type 1 fimbriae expression in verotoxigenic *Escherichia coli*: a comparison between serotypes O157 and O26. Microbiology **147**:145–152.
58. **Erdem AL, Avelino F, Xicohtencatl-Cortes J, Giron JA.** 2007. Host protein binding and adhesive properties of H6 and H7 flagella of attaching and effacing *Escherichia coli.* J. Bacteriol. **189**:7426–7435.
59. **Torres AG, Milflores-Flores L, Garcia-Gallegos JG, Patel SD, Best A, La Ragione RM, Martinez-Laguna Y, Woodward MJ.** 2007. Environmental regulation and colonization attributes of the long polar fimbriae (LPF) of *Escherichia coli* O157:H7. Int. J. Med. Microbiol. **297**:177–185.
60. **Amsler CD, Cho M, Matsumura P.** 1993. Multiple factors underlying the maximum motility of *Escherichia coli* as cultures enter post-exponential growth. J. Bacteriol. **175**:6238–6244.
61. **Zhao K, Liu M, Burgess RR.** 2007. Adaptation in bacterial flagellar and motility systems: from regulon members to 'foraging'-like behavior in *E. coli.* Nucleic Acids Res. **35**:4441–4452.
62. **Arnqvist A, Olsen A, Pfeifer J, Russell DG, Normark S.** 1992. The Crl protein activates cryptic genes for curli formation and fibronectin binding in *Escherichia coli* HB101. Mol. Microbiol. **6**:2443–2452.
63. **Kikuchi T, Mizunoe Y, Takade A, Naito S, Yoshida S.** 2005. Curli fibers are required for development of biofilm architecture in *Escherichia coli* K-12 and enhance bacterial adherence to human uroepithelial cells. Microbiol. Immunol. **49**:875–884.
64. **Kim SH, Kim YH.** 2004. *Escherichia coli* O157:H7 adherence to HEp-2

cells is implicated with curli expression and outer membrane integrity. J. Vet. Sci. **5**:119–124.
65. **Sukupolvi S, Lorenz RG, Gordon JI, Bian Z, Pfeifer JD, Normark SJ, Rhen M.** 1997. Expression of thin aggregative fimbriae promotes interaction of *Salmonella typhimurium* SR-11 with mouse small intestinal epithelial cells. Infect. Immun. **65**:5320–5325.
66. **Uhlich GA, Keen JE, Elder RO.** 2001. Mutations in the *csgD* promoter associated with variations in curli expression in certain strains of *Escherichia coli* O157:H7. Appl. Environ. Microbiol. **67**:2367–2370.
67. **Ogasawara H, Yamada K, Kori A, Yamamoto K, Ishihama A.** 2010. Regulation of the *Escherichia coli csgD* promoter: interplay between five transcription factors. Microbiology **156**:2470–2483.
68. **Han TH, Lee JH, Cho MH, Wood TK, Lee J.** 2011. Environmental factors affecting indole production in *Escherichia coli.* Res. Microbiol. **162**: 108–116.
69. **Cotter PA, Stibitz S.** 2007. c-di-GMP-mediated regulation of virulence and biofilm formation. Curr. Opin. Microbiol. **10**:17–23.
70. **Davies DG, Parsek MR, Pearson JP, Iglewski BH, Costerton JW, Greenberg EP.** 1998. The involvement of cell-to-cell signals in the development of a bacterial biofilm. Science **280**:295–298.
71. **Dorel C, Vidal O, Prigent-Combaret C, Vallet I, Lejeune P.** 1999. Involvement of the Cpx signal transduction pathway of *E. coli* in biofilm formation. FEMS Microbiol. Lett. **178**:169–175.
72. **Martino PD, Fursy R, Bret L, Sundararaju B, Phillips RS.** 2003. Indole can act as an extracellular signal to regulate biofilm formation of *Escherichia coli* and other indole-producing bacteria. Can. J. Microbiol. **49**:443–449.
73. **Weber H, Pesavento C, Possling A, Tischendorf G, Hengge R.** 2006. Cyclic-di-GMP-mediated signalling within the sigma network of *Escherichia coli.* Mol. Microbiol. **62**:1014–1034.
74. **Lehnen D, Blumer C, Polen T, Wackwitz B, Wendisch VF, Unden G.** 2002. LrhA as a new transcriptional key regulator of flagella, motility and chemotaxis genes in *Escherichia coli.* Mol. Microbiol. **45**:521–532.
75. **Brown PK, Dozois CM, Nickerson CA, Zuppardo A, Terlonge J, Curtiss R, III.** 2001. MlrA, a novel regulator of curli (AgF) and extracellular matrix synthesis by *Escherichia coli* and *Salmonella enterica* serovar Typhimurium. Mol. Microbiol. **41**:349–363.
76. **Hengge-Aronis R.** 2002. Recent insights into the general stress response regulatory network in *Escherichia coli.* J. Mol. Microbiol. Biotechnol. **4**:341–346.
77. **Melton-Celsa AR, Rogers JE, Schmitt CK, Darnell SC, O'Brien AD.** 1998. Virulence of Shiga toxin-producing *Escherichia coli* (STEC) in orally-infected mice correlates with the type of toxin produced by the infecting strain. Jpn. J. Med. Sci. Biol. **51**(Suppl):S108–S114.